

# Lawrence Berkeley National Laboratory

## Recent Work

### Title

NEUTRON SPECTRA FROM HEAVY-ION BOMBARDMENT OF GOLD

### Permalink

<https://escholarship.org/uc/item/4zk4x19f>

### Author

Simon, William G.

### Publication Date

1963-04-12

University of California  
Ernest O. Lawrence  
Radiation Laboratory

NEUTRON SPECTRA FROM HEAVY-ION  
BOMBARDMENT OF GOLD

TWO-WEEK LOAN COPY

*This is a Library Circulating Copy  
which may be borrowed for two weeks.  
For a personal retention copy, call  
Tech. Info. Division, Ext. 5545*

## **DISCLAIMER**

This document was prepared as an account of work sponsored by the United States Government. While this document is believed to contain correct information, neither the United States Government nor any agency thereof, nor the Regents of the University of California, nor any of their employees, makes any warranty, express or implied, or assumes any legal responsibility for the accuracy, completeness, or usefulness of any information, apparatus, product, or process disclosed, or represents that its use would not infringe privately owned rights. Reference herein to any specific commercial product, process, or service by its trade name, trademark, manufacturer, or otherwise, does not necessarily constitute or imply its endorsement, recommendation, or favoring by the United States Government or any agency thereof, or the Regents of the University of California. The views and opinions of authors expressed herein do not necessarily state or reflect those of the United States Government or any agency thereof or the Regents of the University of California.

UCRL-10689

UNIVERSITY OF CALIFORNIA  
Lawrence Radiation Laboratory  
Berkeley, California  
Contract No. 7405-eng-48

NEUTRON SPECTRA FROM HEAVY-ION BOMBARDMENT OF GOLD

William G. Simon

April 12, 1963

## NEUTRON SPECTRA FROM HEAVY-ION BOMBARDMENT OF GOLD

William G. Simon

Lawrence Radiation Laboratory  
University of California  
Berkeley, California

April 12, 1963

## ABSTRACT

Neutron yields from bombardment of a thick Au target by 164- and 142-MeV  $O^{16}$  ions have been measured. Neutrons were detected by means of nuclear emulsions at 15-deg intervals from 0 to 165 deg. The yields at 164 and 142 MeV are subtracted to obtain average cross sections over this energy interval which are then transformed to the center-of-mass system. The anisotropy coefficient  $a$ , defined by the expression  $W(\theta) = 1 + a \cos^2 \theta$ , is about 1 for 2-MeV neutrons and decreases rapidly with energy. The distribution of neutrons is essentially isotropic above 6 MeV. This behavior disagrees with calculations of the angular distribution of neutrons from fission fragments, which are based on the fragment angular distribution measured by Viola. It is concluded that some neutrons are emitted from the system before fission occurs.

## NEUTRON SPECTRA FROM HEAVY-ION BOMBARDMENT OF GOLD\*

William G. Simon

Lawrence Radiation Laboratory  
University of California  
Berkeley, California

April 12, 1963

## I. INTRODUCTION

The energy and angular distributions of neutrons from the bombardment of Au by  $O^{16}$  ions have been investigated. Neutron yields from 164- and 142-MeV  $O^{16}$  ions were measured at 15-deg intervals from 0 to 165 deg. We detected neutrons of from 1- to 10-MeV by means of nuclear emulsions, using the internal-radiator method. Average cross sections from 142 to 164 MeV obtained by subtracting the yields are transformed to the compound-nucleus system. The 0 deg yields are extended to 25-MeV neutron energy by using an external radiator together with nuclear emulsions for neutron detection.

## II. EXPERIMENTAL ARRANGEMENT

A. Internal-Radiator Method

The experimental arrangement is shown in Fig. 1. The  $O^{16}$  ions left the accelerator with an energy of 166 MeV. The object was to obtain a well collimated beam of small profile at the target, and at the same time minimize neutron background originating from beam hitting any matter other than the target. A 4-in. quadrupole lens forms the main part of the system. The object for this lens was a 1-in.-diam collimator placed near the Hilac exit. Another 1-in.-diam carbon collimator was placed 21 in. in front of the quadrupole. This eliminated all beam particles

that would strike the beam pipe at a point closer to the target. This collimator was located 175 in. from the emulsion detectors, so that the solid-angle factor for neutrons originating in it was very small. In addition to the solid-angle factor, about 3.5 ft of paraffin shielded the emulsions from this background source.

In order to tune the beam, a quartz crystal with a thin aluminum foil on the beam side was placed in the target position and viewed from the downbeam side with a television camera. The foil and crystal formed the back of a Faraday cup, so that one could measure the beam while viewing the crystal. The accelerator was tuned and the quadrupole lens set to achieve a minimum beam size on the crystal. The beam diameter measured in this way was  $\leq 1/4$  in. The beam pattern at the target was observed several times between runs, and no changes were detected. If the quadrupole lens is adjusted to form a parallel beam, then the position of the beam at the target is insensitive to the position of the beam in the object diaphragm; thus any wandering of the beam exiting from the Hilac would not alter the position of the beam at the target. A 0.1 mil Al foil placed at the Hilac exit stripped the ions to a known charge distribution ( $\approx 98\%$  have charge 8).

The beam was measured by using a Faraday cup. The cup was a 2-3/4-in.-diam by 15-in.-long tube with 1/32-in. walls, insulated from the beam pipe by teflon insulators specially shaped to reduce leakage current. The rear end of the tube was cut at 60 deg to its axis, and a brass ring soldered on to support the targets. The thick ( $132.5 \text{ mg/cm}^2$ ) Au target formed the back of the Faraday cup. Beam energy was determined by measuring the range of the ions in nuclear emulsion, using the range-energy relation of Heckman et al.<sup>1</sup>

### B. Neutron Detection

We detected neutrons by means of nuclear emulsions, using the internal-radiator method. The 1- by 3-in. glass-backed emulsions were placed 8 in. from the target at 15-deg intervals from 0 to 165 deg. The plane of the emulsion contained the radial line from the target, and the 3-in. edge was perpendicular to this line. The 1/32-in. brass front covers of the cameras stopped most of the charged particles from the target. The emulsions used were 600- $\mu$  Ilford types K-2 and K-5. In some cases the plates were exposed in pairs with the emulsion faces together. This greatly reduced the flux of charged particles entering the surface of the emulsion, thus increasing the ease of scanning.

### C. External Radiator Experimental Arrangement

The experimental arrangement for measuring neutron yields by using an external radiator is shown in Fig. 2. The beam geometry was similar to that in the internal-radiator setup, except that the quadrupole-to-target distance was shorter. The beam was measured by using a Faraday cup. The thick Au target, which formed the back of the Faraday cup, was backed by a 3/32-in.-thick piece of lead, which stopped charged particles originating in the target. A polyethylene radiator was placed 14 in. from the target in the forward direction. Nuclear emulsions located 6 in. from the radiator at angles from 20 to 30 deg to the beam direction were used to detect the recoil protons. The polyethylene shield in Fig. 2 protected the emulsions from neutrons coming directly from the target, which would blacken the emulsion if not attenuated.

In order to test for background, the polyethylene radiator was replaced by a thin carbon radiator having the same number of C atoms per  $\text{cm}^2$ . Since all measured protons are assumed to come from n-p collisions in the radiator, runs with the carbon radiator served to measure the background.

### III. EMULSION SCANNING AND DATA ANALYSIS

In the internal-recoil method, the analysis is based on the neutron-proton collisions occurring within the emulsion. If the direction of the incoming neutron is known, then its energy can be calculated from

$$E_n = E_p(R) / \cos^2 \theta, \quad (1)$$

where  $E_p(R)$  is the energy of the recoil proton, and  $\theta$  is the angle between the neutron and proton directions.

The usual method of analysis is to choose a small cone of acceptance, requiring that all measured tracks have angles  $\theta$  less than some maximum angle  $\theta_m$ . Then, instead of calculating  $\cos\theta$  for each track, average values are used. This requires that  $\theta_m$  be less than about 15 deg. This procedure greatly reduces the difficulty of scanning and analysis. A severe disadvantage is that the small cone of acceptance results in a large error in determining which tracks lie within the cone.

In this work, a coordinate readout microscope was used in scanning the plates. The spatial coordinates of a point on a track were automatically recorded on IBM cards, and the analysis was carried out by a computer. The energy of each neutron was calculated according to Eq. (1). This allows the use of a large cone of acceptance (57 deg was used) and thus eliminates a major source of error.

The neutron yield  $Y$  at lab angle  $\theta$  and neutron energy  $E_n$  is

$$Y = \frac{F(E_n, \theta)}{r^2 N},$$

where  $F(E_n, \theta)$  is the flux per unit solid angle,  $r$  is the target to detector distance, and  $N$  is the total number of beam particles.

The yields were measured at beam energies of 164 and 142 MeV. The average cross section over this range of beam energies is obtained by subtracting the yields and dividing by the effective number of target atoms. Thus we have

$$\frac{d^2\sigma}{d\Omega dE} = \frac{Y_1(E_n, \theta) - Y_2(E_n, \theta)}{[R(E_2) - R(E_1)] N_0/A},$$

where  $Y_1$  and  $Y_2$  are the yields at 164 and 142 MeV, respectively, and  $A$  is the mass of a target atom in amu.

The c.m. cross sections are estimated to have an error of about 16% resulting from systematic errors; that is, the overall normalization is estimated to be within 16%. Systematic errors considered in this estimate include errors in the target-to-emulsion distance, beam integration, and the shrinkage factor and hydrogen content of the emulsion.

The presence of background neutrons is easy to detect from the following considerations. (a) Let the polar axis be the target-to-emulsion line. Then the recoil protons must be distributed uniformly with respect to the azimuthal angle and the  $\cos^2$  of the polar angle. (2) All recoil protons must be going away from the target. For protons with energy greater than  $\approx 2$  MeV, the direction of motion can be determined and this test applied. The background estimated by using these methods is  $\lesssim 3\%$  of the total neutron flux.

#### RESULTS AND DISCUSSION

The 0 deg yields for 164-MeV ions obtained by both internal and external methods are shown in Fig. 3. The internal radiator points are typical of those obtained at all angles. The errors shown are statistical errors in the number of tracks measured.

The yields at each lab angle were fit to the form

$$Y(\tau) = A\tau^B \exp(C\tau + D\tau^2),$$

where  $\tau$  is the neutron energy. The c.m. transformations were then done in the following way: A c.m. energy was chosen; then for each lab angle, the lab energy and the corresponding c.m. angle were calculated. The c.m. cross section at the calculated c.m. angle was then found from

$$\frac{\sigma_{\text{c.m.}}(\tau_{\text{c.m.}}, \theta_{\text{c.m.}})}{\sqrt{\tau_{\text{c.m.}}}} = \frac{\sigma_{\text{lab}}(\tau_{\text{lab}}, \theta_{\text{lab}})}{\sqrt{\tau_{\text{lab}}}}$$

The velocity of the compound system used was an average value calculated for  $O^{16}$  ions with energies between the limits of the beam energy (142 and 164 MeV).

The resulting c.m. angular distributions are shown in Fig. 4. The curves are least-square fits to the form  $\sigma(\theta) = \sigma(90 \text{ deg})(1 + a \cos^2 \theta)$ . A summary of values of  $\sigma(90 \text{ deg})$ ,  $a$ , and the cross section averaged with respect to angle is given in Table I. There is no evidence of forward peaking. In fact, there seems to be a tendency to peak backwards. This could be a result of incomplete momentum transfer to the compound system. For those reactions with incomplete momentum transfer, the velocity of the system would be overestimated, with the result that neutrons would appear to be peaked backwards in the compound system. Sikkeland et al.<sup>3</sup> have observed that incomplete momentum transfer occurs in a significant fraction of heavy-ion-induced fission reactions.

Figure 5 shows an experimental plot of  $\sigma_a/E^{1/2}$ . This form plots as a straight line rather than the  $\sigma_a/E$  form expected from a Weisskopf distribution, because the spectra result from multiple emission. The energy

spectra of particles from an evaporation chain has been investigated by LeCouteur.<sup>4</sup> He finds that for an assumed dependence of the temperature on the excitation energy  $T \propto \sqrt{U}$ , there results for a neutron chain

$$F(E) \propto E^{5/11} \exp\left(-\frac{11}{12} \frac{E}{T_n}\right)$$

where  $T_n$  is the temperature governing the first evaporation. This form differs only slightly from that used in this analysis. The observed results are well represented by

$$\sigma_a(E) = 433 E^{1/2} e^{-E/2.01} \text{ mb/MeV-sr}.$$

Integration over energy and angle gives a total cross section of 14 barns for neutron production. The ratio of the number of neutrons for these measurements to the number expected at 164 MeV is calculated to be 0.82. In this calculation we use the cross sections of Thomas<sup>5</sup>, and assume that one additional neutron results from an increase of 11 MeV in excitation energy. The value for comparison, 17.1, lies between the values of 12.8 and 19.2 barns given by Hubbard et al.<sup>6</sup> for carbon and neon on Au.<sup>6</sup> It is somewhat below the value of 25 barns given by Brock,<sup>7</sup> but because of the large normalization errors, the values are not inconsistent.

The observed anisotropy decreases strongly with increasing neutron energy. The last neutron emitted is expected to be more strongly coupled to the angular momentum of the compound system than neutrons from early stages of the evaporation chain. This effect has been observed by Allen<sup>8</sup> and discussed by Douglas and McDonald,<sup>9</sup> and by Ericson.<sup>10</sup> Thus, the lower-energy neutrons are expected to be more anisotropic. This effect could be greatly enhanced if the last pre-fission neutron and the last post-fission neutron from each fragment were strongly coupled to the angular momentum.

Measured angular distributions of fission fragments from heavy-ion-induced fission show large anisotropies. For 164-MeV  $O^{16}$  ions on Au, the forward-to-90-deg ratio is about four.<sup>11,12</sup> This anisotropy affects the angular distribution of neutrons evaporated from the fragments, and thus presents a possibility of separating pre- and post-fission neutrons. Assuming a simple isotropic spectrum in the fragment rest frame and fragments of a single velocity, we can calculate the angular distribution of the neutrons in the compound system. The actual distribution of neutrons from the fragments should show anisotropies greater than those calculated, because neutrons are expected to be evaporated preferentially in the direction of the fragment's motion.

Calculations were made for distributions of the Weisskopf form

$$F(E) \propto E e^{-E/T}$$

and Maxwell form

$$F(E) \propto E^{1/2} e^{-E/T}$$

with temperatures of 1.5 and 2.0 MeV. First the distribution was transformed to a coordinate system at rest with the compound system and with the polar axis in the direction of fragment motion. Then a rotation was made to align the polar axis with the beam direction, and an integration over the fragment angular distribution was done. The results are shown in Fig. 6.

If curve D is the correct one, then the observed distribution at 8 MeV is flatter than the calculated one by only 1.1 standard deviations. However, this curve with  $T = 2.0$  MeV leads to an average neutron energy of 4.7 MeV, which is considerably higher than the observed value of 3.01. To obtain agreement with the average neutron energy, one must assume a temperature

of 1.5 MeV, which results in the more anisotropic curve A. This curve has a value of  $\mu$  which disagrees with the observed value by three standard deviations. This argument is summarized in Table II. It is seen that no value of the temperature can make both the anisotropy and the average neutron energy coincide with experiment. Therefore, it seems reasonable to conclude that a large fraction of the neutrons are evaporated before fission occurs. This result agrees with the considerations of Blann,<sup>13</sup> who finds that the assumption of pre-fission neutron emission is necessary for agreement with the experimentally determined energy required to remove a neutron from the system.

#### FOOTNOTE AND REFERENCES

- \* This work done under the auspices of the U. S. Atomic Energy Commission.
1. H. H. Heckman, B. L. Perkins, W. G. Simon, F. M. Smith, and W. H. Barkas, Phys. Rev. 117, 545 (1960).
  2. L. Rosen, Nucleonics 11, 38 (1953).
  3. T. Sikkeland, E. L. Haines, and V. E. Viola, Jr., Phys. Rev. 125, 1350 (1962).
  4. K. J. LeCouteur, Proc. Phys. Soc. (London) A65, 718 (1952).
  5. T. D. Thomas, Phys. Rev. 116, 703 (1959).
  6. E. L. Hubbard, R. M. Main, and R. V. Pyle, Phys. Rev. 118, 507 (1960).
  7. H. W. Brock, Phys. Rev. 124, 233 (1961).
  8. P. L. Allen, Nuclear Phys. 10, 348 (1959).
  9. A. C. Douglas and N. MacDonald, Nuclear Phys. 13, 382 (1959).
  10. T. Ericson, Advan. Phys. 9, 425 (1960).

11. Victor E. Viola, Jr., Thesis, Lawrence Radiation Laboratory Report UCRL-9610, March 24, 1961 (unpublished).
12. H. C. Britt and A. R. Quinton, Reactions Between Complex Nuclei (John Wiley and Sons, Inc., New York, N. Y., 1960).
13. H. Marshall Blann, Thesis, Lawrence Radiation Laboratory Report UCRL-9190, May 23, 1960 (unpublished).

Table I. Values of the cross section at 90 deg, the anisotropy, and the cross section averaged over the angle for various values of E.

E	$\sigma(90 \text{ deg})$ (mb)	a	Average cross section $\sigma_a = \sigma(90 \text{ deg}) + a/3$
1.5	183 ±39	1.05 ±.32	247
2	176 ±37	0.81 ±.32	224
4	119 ±14	0.159±.19	125
6	53.8±4.5	0.047±.145	55
8	21.9±2.1	0.099±.158	22.7

Table II. Comparison of calculated and observed values of the average neutron energy and the anisotropy  $a$ . No assumed value of  $T$  can make both these parameters consistent with the observed values.

Assumed distribution in fragment rest frame		$\langle E_f \rangle$	Resulting distribution in compound-system frame	
				$\langle E_{c.s.} \rangle$
Weisskopf	$F(E) \propto E e^{-E/T}$	$2T$	Feather	$E_f + 2T$
Maxwell	$F(E) \propto E^{1/2} e^{-E/T}$	$3/2 T$	Watt	$E_f + 3/2 T$

$E_f = 0.71,$		$F(\theta) = 1 + a \cos^2 \theta$	
---------------	--	-----------------------------------	--

		$\langle E_{c.s.} \rangle$	$a$ (8 MeV)
Curve A	Maxwell - 1.5 MeV	2.96	0.56
B	Weisskopf- 1.5 MeV	3.71	0.46
C	Maxwell - 2.0 MeV	3.71	0.37
D	Weisskopf- 2.0 MeV	4.71	0.28
	Observed value	3.01	0.099±.158

FIGURE LEGENDS

Fig. 1. Experimental arrangement for neutron detection with emulsion used as both detector and radiator.

Fig. 2. Experimental arrangement for neutron detection using an external polyethylene radiator.

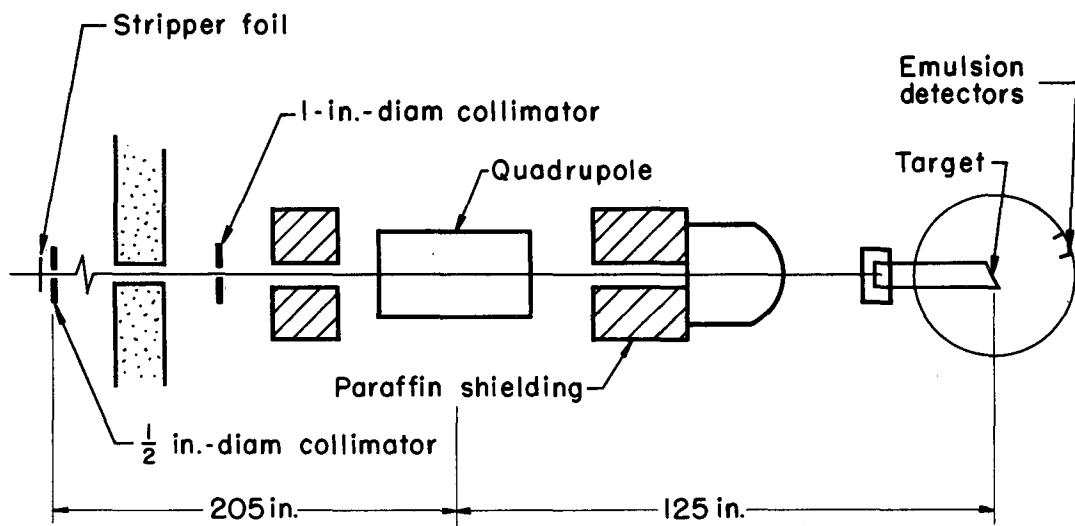
Fig. 3. Neutron yield in the laboratory system at 0 deg for 164-MeV  $O^{16}$  ions on a thick Au target. Triangles and circles designate points obtained using internal- and external-radiator methods.

Fig. 4. Center-of-mass angular distributions for neutrons.

Fig. 5. "Temperature" plot for cross sections averaged over angle. The line shown is

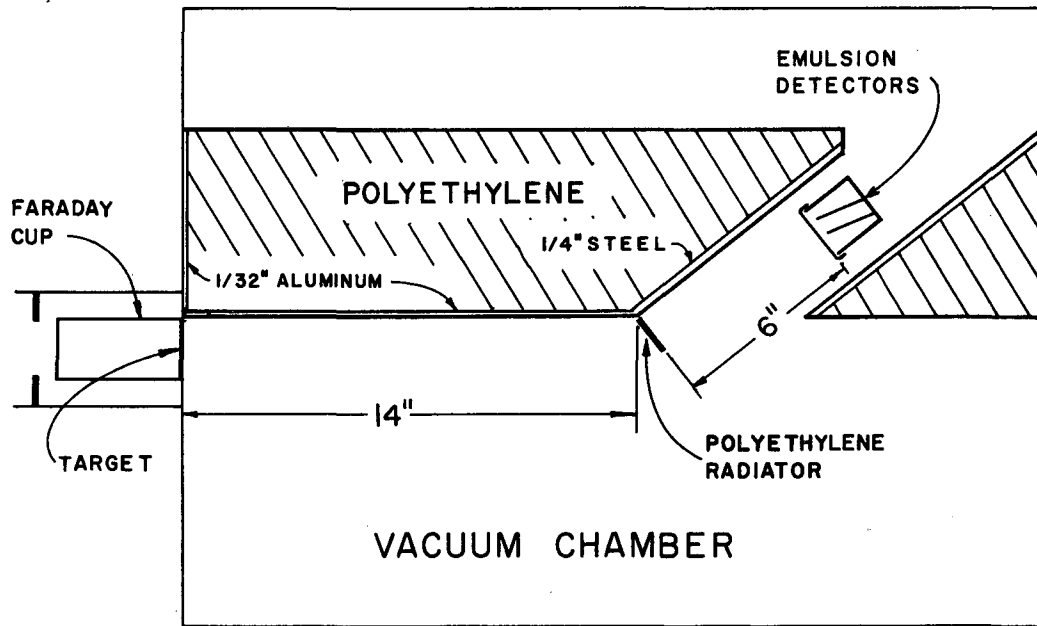
$$\frac{d^2\sigma}{d\Omega dE} = 433 E^{1/2} e^{-E/2.01} \text{ mb/MeV-sr} .$$

Fig. 6. Neutron angular distributions calculated assuming post-fission emission. Curves A and C are for Maxwell distributions with  $T = 1.5$  and 2 MeV; B and D are for Weisskopf distributions at 1.5 and 2 MeV.



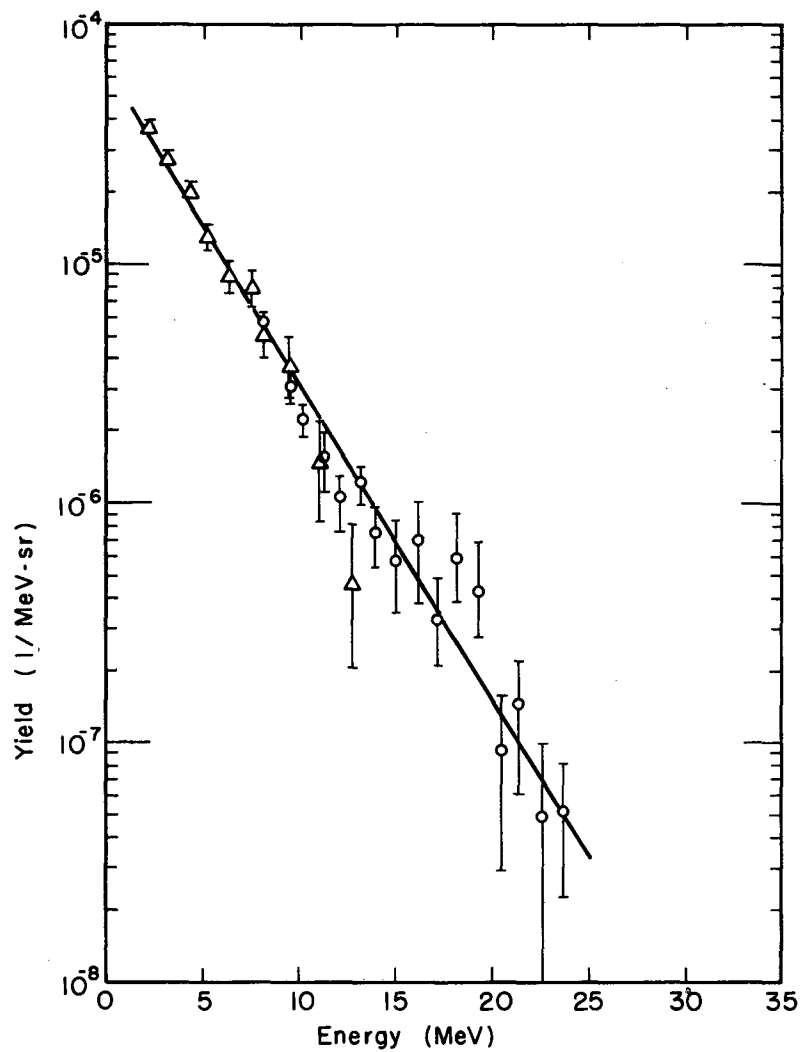
MU-30018

Fig. 1



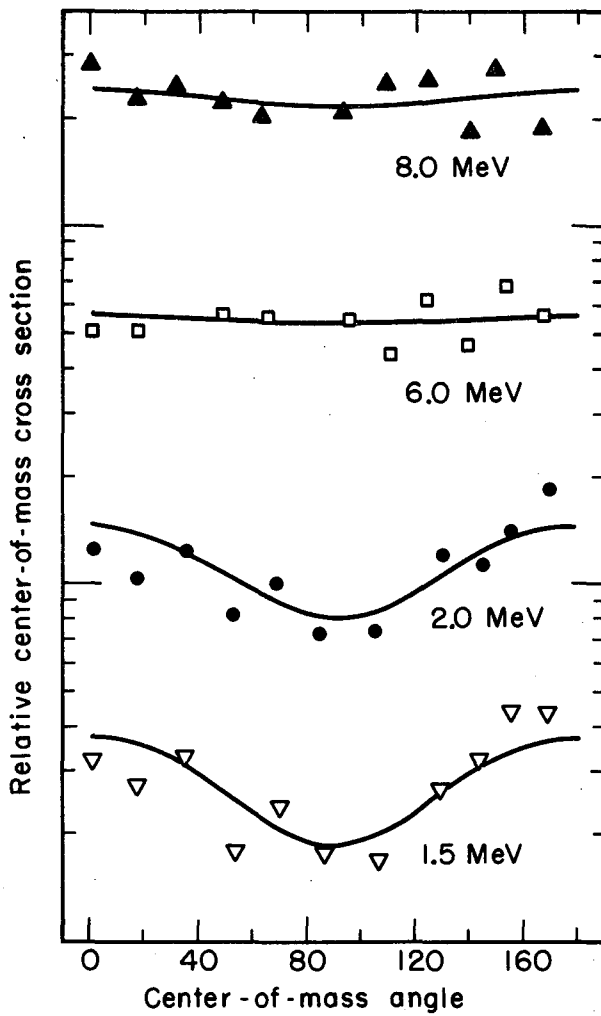
MU-30019

Fig. 2



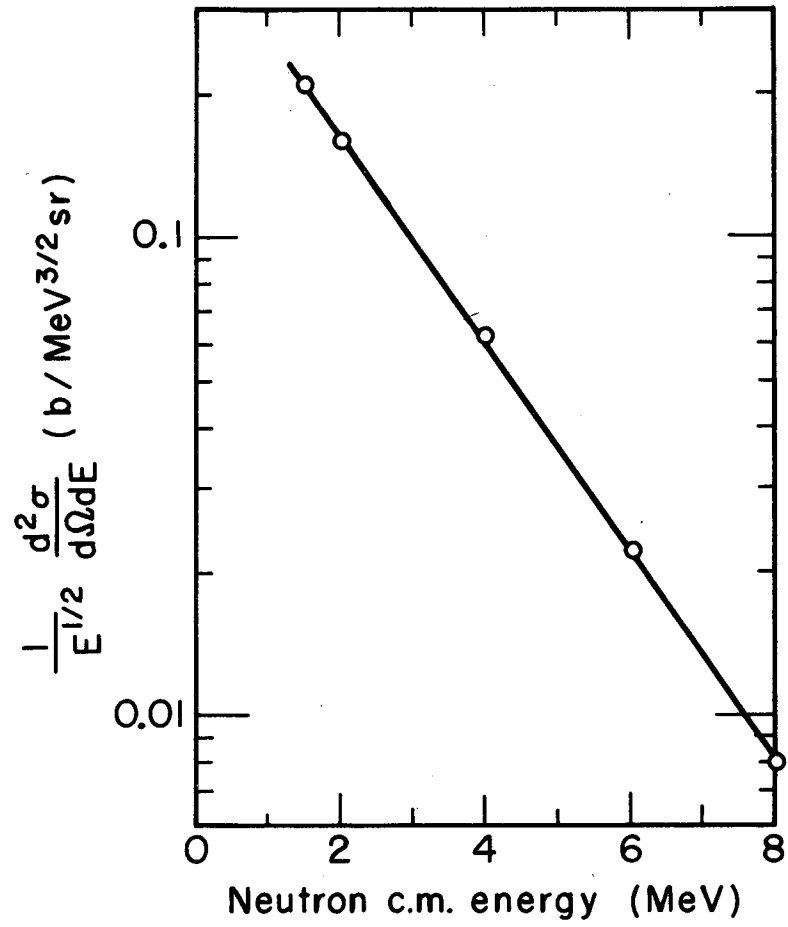
MU-30021

Fig. 3



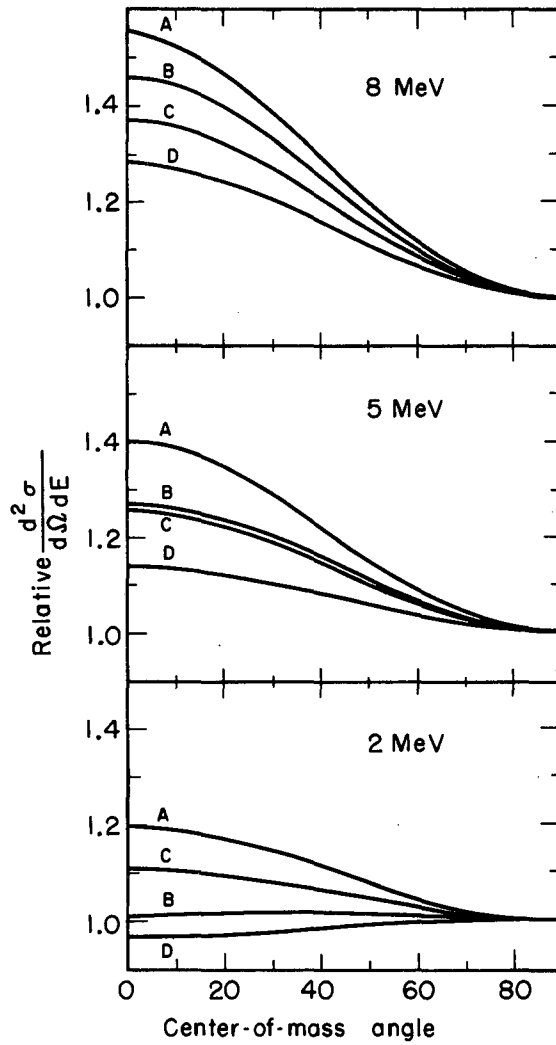
MU-30017

Fig. 4



MU-30016

Fig. 5



MU-30020

Fig. 6

This report was prepared as an account of Government sponsored work. Neither the United States, nor the Commission, nor any person acting on behalf of the Commission:

- A. Makes any warranty or representation, expressed or implied, with respect to the accuracy, completeness, or usefulness of the information contained in this report, or that the use of any information, apparatus, method, or process disclosed in this report may not infringe privately owned rights; or
- B. Assumes any liabilities with respect to the use of, or for damages resulting from the use of any information, apparatus, method, or process disclosed in this report.

As used in the above, "person acting on behalf of the Commission" includes any employee or contractor of the Commission, or employee of such contractor, to the extent that such employee or contractor of the Commission, or employee of such contractor prepares, disseminates, or provides access to, any information pursuant to his employment or contract with the Commission, or his employment with such contractor.

